Fan *et al. Alzheimer's Research & Therapy* (2025) 17:122
https://doi.org/10.1186/s13195-025-01769-9

Alzheimer's Research & Therapy

RESEARCH Open Access

Compositional and functional gut microbiota alterations in mild cognitive impairment: links to Alzheimer's disease pathology

Kang-Chen Fan[1], Chen-Ching Lin[2], Yen-Ling Chiu[3,4,5], Seong-Ho Koh[6,7], Yi-Chien Liu[8] and Yi-Fang Chuang[1,9,10*]

Abstract

Background Emerging evidence highlights the bidirectional communication between the gut microbiota and the brain, suggesting a potential role for gut dysbiosis in Alzheimer's disease (AD) pathology and cognitive decline. Existing literature on gut microbiota lacks species-level insights. This study investigates gut microbiota alterations in mild cognitive impairment (MCI), focusing on their association with comprehensive AD biomarkers, including amyloid burden, tau pathology, neurodegeneration, and cognitive performance.

Methods We analyzed fecal samples from 119 individuals with MCI and 320 cognitively normal controls enrolled in the Taiwan Precision Medicine Initiative on Cognitive Impairment and Dementia cohort. Shotgun metagenomic sequencing was conducted with taxonomic profiling using MetaPhlAn4. Amyloid burden and plasma pTau181 were quantified via PET imaging and Simoa assays, respectively, while APOE genotyping was performed using TaqMan assays. Microbial diversity, differential abundance analysis, and correlation mapping with neuropsychological and neuroimaging measures were conducted to identify gut microbiota species signatures associated with MCI and AD biomarkers.

Results We identified 59 key microbial species linked to MCI and AD biomarkers. Notably, species within the same genera, such as *Bacteroides* and *Ruminococcus*, showed opposing effects, while *Akkermansia muciniphila* correlated with reduced amyloid burden, suggesting a protective role. Functional profiling revealed microbial pathways contributing to energy metabolism and neuroinflammation, mediating the relationship between gut microbes and brain health. Co-occurrence network analyses demonstrated complex microbial interactions, indicating that the collective influence of gut microbiota on neurodegeneration.

Conclusions Our findings challenge genus-level microbiome analyses, revealing species-specific modulators of AD pathology. This study highlights gut microbial activity as a potential therapeutic target to mitigate cognitive decline and neurodegeneration.

Keywords Gut-brain axis, Gut microbiome, Alzheimer's disease pathology, Mild cognitive impairment, Shotgun metagenomics, Amyloid PET, Plasma pTau181, APOE

*Correspondence:
Yi-Fang Chuang
chuangy@nycu.edu.tw

Full list of author information is available at the end of the article

Background

Alzheimer's Disease (AD), the most common cause of dementia, is characterized by progressive cognitive decline and hallmark pathologies, including extracellular amyloid-beta (Aβ) plaques and intracellular tau protein neurofibrillary tangles. Mild Cognitive Impairment (MCI), an intermediate stage between normal cognition and dementia, is a clinically heterogeneous condition marked by noticeable cognitive deficits that do not significantly interfere with daily activities. Recognized as a critical stage in the AD continuum, MCI carries a significantly higher risk of progression to AD annually [1]. Recent advancements in biomarkers reflecting AD pathology—such as amyloid deposition and tau protein hyperphosphorylation—have revolutionized the research framework and diagnostic criteria for AD. In 2018, the National Institute on Aging and Alzheimer's Association (NIA-AA) introduced the AT(N) framework, categorizing biomarkers into amyloid pathology (A), tau pathology (T), and neurodegeneration (N) [2]. This framework provides a biological basis for describing and defining AD, enabling researchers to determine whether an individual falls within the AD spectrum and, if so, their status along the disease continuum based on combined AT(N) profiles and cognitive stages.

For decades, amyloid hypothesis has been central to AD research, guiding treatment strategies aimed at targeting amyloid-beta (Aβ) [3]. While amyloid-lowering therapies are beginning to show promise, their effectiveness and generalizability continue to be subjects of debate. Although robust in vivo biomarker evidence supports an amyloid cascade driving cognitive decline, the hypothesis alone does not fully explain the complexity of AD. The heterogeneity of dementia suggests that additional factors, such as coexisting brain pathologies, systemic inflammation, and host resilience, play significant roles in disease progression [4]. Emerging evidence highlights the bidirectional relationship between the gut microbiota and the central nervous system, referred to as the microbiota-gut-brain axis. Dysbiosis—a disruption in gut microbial composition—has been implicated in neurodegenerative conditions, including AD, through mechanisms involving systemic inflammation, blood-brain barrier permeability, and direct modulation of amyloid and tau pathologies [5, 6]. Furthermore, altered microbial diversity and composition have been observed across the clinical spectrum of AD, including MCI, suggesting that gut microbiota may serve as a critical factor in the multifaceted processes driving cognitive decline.

Findings indicate an increase in pro-inflammatory *Bacteroidetes* and a decline in protective *Firmicutes* and *Faecalibacterium* in MCI [7]. While some studies have reported gut microbial profiles distinguishing MCI from healthy controls and AD, variability in diagnostic criteria, study design, and analytical methods has led to conflicting results. Additionally, most of these studies rely on 16 S rRNA sequencing, which limits resolution to the genus level, preventing the identification of specific bacterial species that may play key roles in disease mechanisms [6, 7]. Moreover, there are limited studies with small sample sizes exploring the relationship between gut microbiota data with comprehensive AD biomarker profiles [8–12].

This study addresses these gaps by investigating the relationship between gut microbiota composition and function with a comprehensive range of AD biomarkers, including amyloid burden, tau pathology, and neurodegeneration. Utilizing shotgun metagenomics and multimodal biomarker assessments in a well-characterized MCI population, we aim to elucidate the microbial signatures and underlying mechanisms that drive cognitive decline and AD progression.

Materials and methods

Study design and participants

This study utilized baseline data in the Taiwan Precision Medicine Initiative on Cognitive Impairment and Dementia Cohort (TPMIC), a prospective, dynamic cohort study designed to develop a comprehensive biobank comprising blood biomarkers, gut microbiota, genetic profiles, neuroimaging, and clinical data linked to cognitive impairment. The TPMIC recruited adults aged 50 years and older from community and hospital settings in northern Taiwan. Hospital-based participants were drawn from health checkup centers as well as psychiatry and neurology outpatient clinics in both Far Eastern Memorial Hospital and Cardinal Tien Hospital. Exclusion criteria included older adults with life expectancy under six months, recent surgery, or major psychiatric or neurological disorders unrelated to the dementia spectrum. Ethical approval was obtained from the Far Eastern Memorial Hospital Research Ethics Committee (110065-F) and the Institutional Review Board of Cardinal Tien Hospital (CTH-110-2-1-014), with informed consent secured from all participants.

The TPMIC cohort includes individuals with normal cognitive function, MCI, or AD. Diagnoses of MCI and AD were determined by an expert panel comprising a psychiatrist, a neurologist, and a clinical psychologist, following the NIA-AA criteria [2, 13]. At each cohort visit, all participants were invited to provide a fresh fecal sample. In this study, only individuals with MCI and cognitively normal controls were included. Between August 2021 and October 2023, 119 adults with MCI and 320 cognitively normal adults, all with available gut microbiota profiles, were included in this study.

Metagenomic sequencing data processing and quality control

Each participant collected one fresh fecal sample and mailed it to AllBio Biotechnology Corp. (Taichung, Taiwan). DNA extraction, sequencing, library construction of amplicon DNA samples, and quality control were entrusted to AllBio Life (Taichung, Taiwan). DNA was extracted using DNeasy PowerSoil Pro Kit (Qiagen, MD, USA). The preparation of next generation sequencing library was constructed using the VAHTS Universal Pro DNA Library Prep Kit for Illumina (#ND608, Vazyme, Nanjing, China). Genomic DNA (200 μg) was randomly fragmented to an average size of 300–350 bp using a Covaris ultrasonicator system (Covaris, Woburn, USA). End repair and adaptor ligation were then performed with End Prep Enzyme Mix, which added adaptors to both the 5' and 3' ends of the fragments. DNA Cleanup beads were then utilized to select appropriately sized adaptor-ligated fragments for sequencing. Subsequently, each sample was amplified with P5 and P7 primers for 8 cycles; these primers facilitate annealing to the flow cell for bridge PCR, with the P7 primer containing a six-base index for sample multiplexing. PCR products were purified and validated using an Agilent 2100 Bioanalyzer (Agilent Technologies, Santa Clara, USA), and the final libraries were sequenced as paired-end 150 bp reads on the Illumina Novaseq platform (Illumina, San Diego, USA).

To ensure the metagenomic sequencing data met the required standards for downstream analysis, a series of quality control (QC) steps were applied using Cutadapt version 1.9.1 [14]. Initially, extraneous sequences—such as primers and adapters introduced during library preparation—were removed to avoid interference with subsequent analyses. Reads were then filtered by their Phred quality score, an indicator of base-calling accuracy, with reads scoring below 30 at either end discarded to eliminate low-quality, error-prone data. Further filtering steps removed reads containing an excessive number of N bases as well as reads shorter than 75 base pairs, thereby ensuring that only high-quality reads were retained. Finally, host sequences were removed by aligning reads to the NCBI GRCh38 human reference genome using Bowtie2 version 2.2.5 [15], filtering out any human DNA present in the samples, resulting in FASTQ files comprised exclusively of metagenomic sequences relevant for analysis.

The taxonomic composition of the metagenomic sequencing data was analyzed using MetaPhlAn4 (v4.0.6) pipeline [16] and its default database mpa_vOct22_CHOCOPhlAnSGB_202212. The MetaPhlAn4 pipeline initiates by aligning raw metagenomic sample reads to a species-level genome bin (SGB) marker database via Bowtie2. In the database, SGBs include both known species (kSGBs) and yet-to-be-characterized species (uSGBs), which are defined solely based on metagenome-assembled genomes (MAGs). We added "–ignore_usgbs" in the parameter so as not to profile currently unknown equivalent clades. Despite that, the default MetaPhlAn4 parameters were applied, enabling precise classification and valuable insights into the microbial community composition of the samples. The taxonomy and relative abundance table were imported into R for further analysis using the Phyloseq package [17]. Read counts were calculated by multiplying the total sequence reads by the relative abundance of each taxon.

Cognitive assessment and brain structure analysis

A comprehensive neuropsychological test battery was used in the TPMIC cohort to evaluate global cognition and specific cognitive domains, including attention, memory, executive functions, and language. All tests were administered in Chinese. Global cognitive status was measured using the Mini-Mental State Examination (MMSE). Attention was assessed with the Color Trails Test 1 (CTT1), Digit Span subtests (DS), Digit Symbol Substitution Test (DSST), and immediate recall from the Logical Memory subset (LMI) of the Wechsler Memory Scale. The memory domain was evaluated with the delayed recall task of the Logical Memory subset (LMII). Executive function was assessed using the Color Trails Test 2 (CTT2), Semantic Verbal Fluency (VF), and the interference score of Stroop Color and Word Test (SCWT). Language function was rated by uncued response to the 30-item Boston Naming Test (BNT). All test scores were z-transformed, and the mean z-scores for each cognitive domain were calculated to generate composite scores.

Each participant underwent imaging on a 3T MRI scanner equipped with a 16-channel head coil (MAGNETOM Skyra, Siemens Healthcare, Erlangen, Germany). High-resolution T1-weighted images were acquired using the magnetization-prepared rapid-acquisition gradient echo (MPRAGE) protocol [18], and diffusion tensor imaging (DTI) parameters were aligned with those specified by Chiu et al. (2019).

For the T1-weighted imaging analysis, data processing was conducted using Freesurfer version 7.4.1 (http://surfer.nmr.mgh.harvard.edu/) [19], involving skull stripping, cortical surface reconstruction, automated labeling, cortical parcellation, and subcortical segmentation (aparc + aseg). Manual corrections were applied where topological defects were identified at the pia mater or gray-white matter boundaries. Volumetric data were extracted for key brain regions, including total brain volume, ventricles, gray matter (GM), white matter (WM), and specific regions of interest (ROIs) such as the hippocampus and entorhinal cortex, which are relevant to AD

and MCI. To account for individual differences in cranial volume, estimated total intracranial volume (eTIV) was applied. Additionally, cortical thickness in nine AD-related regions was calculated based on prior research [20] (Supplementary Table S1). The volume for each region was derived by multiplying thickness by surface area, and an AD cortical thickness score (AD-CTS) was computed by dividing the cumulative volume of AD signature regions by the total surface area to represent the average cortical thickness associated with AD.

For DTI analysis, data preprocessing was carried out using the PANDA toolbox (version 1.3.1) in MATLAB, integrated with the FMRIB Software Library (FSL, version 6.0, University of Oxford, UK) [21]. A brain mask was applied to diffusion images for skull stripping using FSL's brain extraction tool, followed by eddy correction to mitigate head motion and eddy current-induced distortions. Diffusion tensors were reconstructed with the DTIFIT command, producing diffusion tensor metrics such as fractional anisotropy (FA). Utilizing the PANDA pipeline's WM atlases, specifically the ICBM-DTI-81 WM labels atlas and the JHU WM tractography atlas, the WM was segmented into multiple ROIs for ROI-based analysis. Building on previous studies investigating AD-related WM tracts [22–24], seventeen ROIs encompassing commissural, projection, and association fibers were selected (Supplementary Table S2), and the mean FA values of these fibers were calculated to construct an AD white matter integrity score (AD-WMIS).

Amyloid-β and pTau assessment

Brain amyloid PET imaging was utilized in this study to assess amyloid burden in participants, with florbetaben serving as the amyloid PET tracer. Amyloid PET positivity was determined through a consensus meeting involving one neurologist and three nuclear medicine specialists. Quantitative analysis of PET images was conducted using PMOD software (version 4.1, PMOD Technologies, Zurich, Switzerland). T1-weighted MRI scans were used to define ROIs based on the Hammers template, which was then superimposed onto dynamic PET scans to extract regional time-activity curves. Nondisplaceable binding potential images were generated using cerebellar gray matter as a reference region. The volume-weighted mean cortical amyloid-β load was subsequently calculated using the Hammers brain atlas, encompassing all cortical regions, including the frontal, temporal, parietal, occipital, and cingulate cortices. Late-phase PET images were collected 50 min after tracer injection, followed by a 20-minute scan to quantify amyloid-β burden. The standardized uptake value ratio (SUVR) was calculated for the entire brain and specific brain regions, including the frontal, parietal, temporal, occipital, cingulate, and insular cortices. A cutoff SUVR value of 1.19 (specificity 91.83%; sensitivity 94.54%) was established using receiver operating characteristic (ROC) analysis, with visual read results serving as the reference standard.

Plasma phospho-Tau 181 (pTau181) levels were measured at Veritas Laboratory (Taipei, Taiwan) using the Simoa Human pTau181 Advantage V2 assay on the Simoa HD-X analyzer, following the manufacturer's protocol. Positivity for pTau181 was determined by binarizing plasma levels based on a Youden index-derived cutoff of 2.565 pg/mL within the dataset.

APOE genotyping

APOE genotyping was conducted by the laboratory of Professor Wei-Chiao Chang at Taipei Medical University. Genomic DNA was extracted from participants' peripheral blood mononuclear cells, and genotyping was performed using the TaqMan Allelic Discrimination Assay (Applied Biosystems, Foster City, CA) for the single nucleotide polymorphisms rs7412 and rs429358. Polymerase chain reaction (PCR) was carried out in a 96-well microplate using an ABI9700 Thermal Cycler (Applied Biosystems). Following PCR amplification, fluorescence signals were measured and analyzed with System SDS software version 1.2.3 (Applied Biosystems).

Biodiversity analysis

To measure overall biodiversity in the gut environment, alpha-diversity indices and beta-diversity matrices were computed with the calculate_diversity.R script from the MetaPhlAn tutorial. Alpha diversity, indicating the average species diversity within a local environment, was assessed using indices such as richness, Gini, Shannon, and Simpson. Differences in alpha diversity between MCI and normal were analyzed with linear regression models adjusted for potential confounders. Beta diversity, reflecting species diversity differences between ecosystems, was quantified using Aitchison, Bray–Curtis, Jaccard, unweighted UniFrac, and weighted UniFrac distances. Principal coordinate analysis (PCoA) was employed to transform data into lower-dimensional space and visualize results of these distance metrics. Differences in beta diversity between MCI and cognitively normal groups were evaluated using PERMANOVA (permutational multivariate analysis of variance) and the Wd* test [25, 26].

Identification of key microbes linked to cognitive impairment through differential abundance analysis and correlation heatmap

Recognizing that MCI represents a heterogeneous clinical stage, we first compared microbiota composition between MCI and cognitively normal individuals to identify global microbial alterations associated with cognitive impairment. We then conducted biomarker-stratified

comparisons within the MCI group, such as A + MCI vs. A – MCI and T + MCI vs. T – MCI, allowing us to isolate microbial changes that may be specifically associated with underlying amyloid or tau pathology. If a microbial species exhibited consistent directional changes across both the general MCI vs. normal cognition comparison and AD biomarker-stratified analyses, we interpreted this as supportive evidence for a potential link between the species and AD-related neurodegenerative processes.

Differential abundance analysis (DAA) was conducted to identify differences in species of interest to pinpoint key microbes potentially involved in cognitive impairment. Comparisons included MCI versus cognitively normal, A + MCI versus A-MCI, T + MCI versus T-MCI, A + T + versus A-T-, and APOE4 + versus APOE4-. The APOE4- group was matched to the APOE4 + group in a 1:2 ratio based on age, gender, and educational level using propensity score matching. Previous studies have highlighted that DAA in microbiome research is often inconsistent and lacks robustness due to the variability in statistical tests, assumptions underlying analysis tools, and dataset characteristics [27]. To address this challenge and better identify genuinely differentially abundant microbes, four widely used methods were applied: linear discriminant analysis (LDA) effect size (LEfSe) [28], Microbiome Multivariable Association with Linear Models (MaAsLin2) [29], ANOVA-like Differential Expression tool (ALDEx2) [30], and metagenomeSeq [31]. Species with a prevalence greater than 0.125 in each comparison dataset were analyzed, and those showing significance in at least two of the four tests were identified as key microbes.

LEfSe employed the Kruskal–Wallis (KW) sum-rank test to identify features with significant differences in abundance, followed by unpaired Wilcoxon rank-sum tests to assess their biological significance across subclasses. MaAsLin2 fitted a linear model to the transformed abundance of each feature based on the specified sample grouping, evaluated significance, and reported Benjamini-Hochberg (BH) false discovery rate (FDR)-adjusted p-values. Both raw models and models adjusted for covariates, including age, gender, and education, were analyzed. ALDEx2 utilized Monte Carlo sampling from Dirichlet distributions, used a uniform prior, applied centered log-ratio (CLR) transformation to the realizations, and calculated expected values for the Wilcoxon rank-sum test and posterior predictive values for Welch's t-test on the transformed data. In metagenomeSeq, cumulative sum-scaling normalization was performed using cumNormStat and cumNorm to normalize sequence counts based on lower-quartile feature abundance. The fitFeatureModel function modeled normalized feature counts using a zero-inflated log-normal model and generated FDR-adjusted p-values.

These key microbes were further analyzed by mapping their results to neuropsychological tests, AD-related brain structures, and WM ROIs. Partial correlations were calculated between the centered-log ratio (CLR)-transformed relative abundance of key microbes and the cognitive and neuroimaging measures from each comparison. Microbes showing significant correlations with both cognitive performance and brain structures were deemed to have the most robust evidence, offering insights into specific species potentially implicated in neurodegeneration.

Mediation analysis of key microbes, microbial metabolic functions, and their impact on cognitive impairments

To further investigate the significant partial correlations identified in the correlation heatmaps, we examined the metabolic functions through which key microbes exert their effects. Microbial functional profiling was performed for each participant using the HMP Unified Metabolic Analysis Network (HUMAnN version 3.8). Mediation analysis was conducted with the CLR-transformed relative abundance of key microbes as the exposure, KEGG Orthology (KO) terms (to which key microbes contribute) as mediators, and outcomes correlated with the key microbes as the dependent variable. The mediation analysis was implemented using an R package for causal mediation analysis [32]. Given the exploratory nature of this study, no multiple comparison adjustments were applied. Statistical significance was determined at a p-value threshold of 0.05 for both the average causal mediation effect (ACME) and the total effect (TE).

Co-occurrence network analysis of key microbes

The interplay among key microbes identified in this study provides valuable insights into gut-brain interactions. The complex relationships among these gut inhabitants involve mutual benefits, cohabitation, competition, and interactions between microbial entities and their metabolites. Microorganisms often function in groups, influencing their environment through synergistic interactions, thereby shaping the structure and diversity of microbial communities. This underscores the importance of conducting network analysis to better understand these interactions. However, network analysis in microbiome studies presents challenges due to the compositional nature of the data, inherent heterogeneity, and sparsity (i.e., numerous zero values) [33–35]. To address these issues, we utilized the NetCoMi package [36], which integrates multiple co-occurrence network analysis methods. Among the available algorithms, SParse InversE Covariance Estimation for Ecological Association Inference (SPIEC-EASI) [37], the Semi-Parametric Rank-based Approach for INference in Graphical models

(SPRING) [38], and gCoda [39] were applied to construct networks tailored to these challenges and metagenomic data. Networks were constructed using these algorithms to uncover distinct microbial interaction patterns associated with cognitive impairment.

Statistical analysis

Descriptive comparisons between MCI and cognitively normal participants were conducted using T-tests for continuous variables and Chi-square tests for binary or categorical variables. Partial correlations were calculated to account for potential confounding factors, adjusting for age, gender, and education in cognitive function analyses, and for age, gender, and eTIV in neuroimaging analyses. All statistical analyses were conducted using R version 4.4.1 and Stata 18, with a significance threshold set at $p < 0.05$ for all tests.

Results

Characteristics of participants

Table 1 summarizes the characteristics of participants with MCI and cognitively normal older adults, along with comparisons between subgroups with amyloid and pTau data. Characteristics of participants across biomarker subgroups are summarized in Supplementary Table S3. For T1-weighted imaging analysis, ten MCI participants and fifteen cognitively normal counterparts were excluded due to missing data, failed MRI scans (e.g., claustrophobia), preprocessing errors, or poor data quality. Similarly, for DTI analysis, five MCI participants and twelve controls were excluded for the same reasons, as detailed in Supplementary Fig. S1.

Participants with MCI were older (73.7 vs. 66.8 years) and had lower educational attainment (10.1 vs. 13.1 years). They also had a higher prevalence of hypertension (52% vs. 38%) and diabetes (28% vs. 18%), with no significant differences in dietary habits. The MCI group exhibited poorer cognitive performance and greater brain structure atrophy compared to cognitively normal participants. Detailed characteristics of biomarker subgroups are provided in Supplementary Table S3. After quality control of metagenomic sequencing data, an average of 3.11×10^7 reads per sample was obtained, with no significant difference between MCI and cognitively normal participants (3.09×10^7 vs. 3.17×10^7, $p = 0.098$). A total of 977 species were identified after profiling across all participants.

Biodiversity differences in the gut microbiome between MCI and normal cognition

Supplementary Fig. S2 shows the alpha diversity comparisons between individuals with MCI and cognitively normal older adults. All indices were comparable between the two groups, reflecting similar biodiversity within each sample. Even after adjusting for covariates such as age, gender, education, hypertension, and diabetes mellitus, no statistically significant differences were observed in the diversity indices of the MCI group (Supplementary Table S4). Beta diversity, visualized through principal coordinate analysis (PCoA), also showed no distinguishable patterns of similarity or dissimilarity between the groups (Supplementary Fig. S3). Each distance matrix revealed undifferentiated clustering patterns, as confirmed by PERMANOVA and Wd* test results ($p < 0.05$) (Supplementary Table S5). In conclusion, the alpha and beta diversity analyses did not reveal significant differences in microbial diversity between participants with MCI and those with normal cognitive function.

Identification of key microbes associated with Alzheimer's pathology and cognitive impairment

After conducting DAA for each comparison, we identified 59 key microbes potentially associated with cognitive decline. Table 2 summarizes the positive or negative associations of these key microbes with amyloid, pTau181, AT status, and APOE4. Details on the comparisons in which these key microbes demonstrated significance are provided in Supplementary Tables S6–S10. Several species exhibited consistent results across comparisons. For instance, *Bacteroides eggerthii*, negatively associated with MCI, A + T +, and APOE4 +, could be considered a beneficial microbe. Similarly, *Akkermansia muciniphila*, a well-known next-generation probiotic, showed a negative correlation with amyloid positivity.

Correlation heatmaps between these microbes and neuropsychological testing, as well as neuroimaging results, provided stronger evidence linking specific species to cognitive impairment, as shown in Fig. 1 and Supplementary Fig. S4. After adjusting for potential confounders, beneficial microbes were positively associated with better cognitive performance, larger overall brain volume, smaller ventricular size, larger key ROIs such as the hippocampus, and higher FA in DTI, reflecting better white matter integrity. These findings suggest that beneficial microbes may play a protective role in maintaining cognitive function and brain health. Conversely, pathogenic microbes were associated with impaired brain function and atrophy in key brain structures, indicating their potential contribution to neurodegeneration.

Mediating role of microbial enzymes in key microbe-cognitive function and brain structure correlations

We investigated key microbes significantly associated with cognitive domains, including attention, executive functions, memory, and language, as well as neuroimaging variables such as total brain volume, ventricular size, GM, WM, hippocampus, entorhinal cortex, AD-CTS, and AD-WMIS. As mediators, we selected KO

Table 1 Characteristics of participants

		Whole sample		Amyloid subgroup		pTau subgroup	
Characteristics		**Normal**	**MCI**	**Normal**	**MCI**	**Normal**	**MCI**
		***N*=320**	***N*=119**	***N*=75**	***N*=70**	***N*=92**	***N*=59**
Age, years, mean ± SD		66.8 ± 6.8	73.7 ± 7.3†	69.7 ± 6.7	75.9 ± 6.3†	67.4 ± 7.3	72.3 ± 8.0†
Male, N(%)		111 (35)	51 (43)	36 (48)	27 (39)	36 (39)	27 (46)
Education, years, mean ± SD		13.1 ± 4.0	10.1 ± 4.8†	13.4 ± 4.3	9.8 ± 4.5†	12.2 ± 3.7	9.0 ± 4.1†
Smoke ever, N(%)		54 (18)	28 (25)	16 (25)	14 (21)	16 (18)	16 (29)
Drink ever, N(%)		87 (29)	34 (30)	18 (28)	15 (23)	26 (30)	17 (30)
BMI, mean ± SD		24.7 ± 3.4	24.3 ± 4.0	24.1 ± 3.5	23.7 ± 3.8	24.7 ± 3.3	24.8 ± 4.0
DM, N(%)		54 (18)	31 (28)*	20 (30)	20 (30)	16 (18)	16 (29)
HTN, N(%)		115 (38)	58 (52)*	22 (34)	33 (50)	29 (34)	26 (47)
Vegetarian, N(%)‡	Non	227 (85)	67 (85)	27 (79)	29 (85)	43 (70)	37 (84)
	Flexitarian	22 (8)	8 (10)	3 (9)	2 (6)	9 (15)	5 (11)
	Vegetarian	19 (7)	4 (5)	4 (12)	3 (9)	9 (15)	2 (5)
Tea consumption, N(%)§	Never	115 (43)	35 (46)	10 (30)	14 (45)	25 (42)	19 (45)
	Sometimes	77 (29)	17 (22)	12 (36)	8 (26)	17 (28)	10 (24)
	Frequently	73 (28)	24 (32)	11 (33)	9 (29)	18 (30)	13 (31)
Coffee consumption, N(%)§	Never	93 (35)	35 (44)	11 (32)	18 (53)	21 (35)	21 (48)
	Sometimes	50 (19)	14 (18)	9 (26)	5 (15)	13 (22)	8 (18)
	Frequently	122 (46)	30 (38)	14 (41)	11 (32)	26 (43)	15 (34)
with Aβ data, N(%)		75 (23)	70 (59)†	-	-	34 (37)	30 (51)
Aβ Status, N(%)	-	65 (87)	30 (43)†	65 (87)	30 (43)†	29 (85)	13 (43)†
	+	10 (13)	40 (57)	10 (13)	40 (57)	5 (15)	17 (57)
with pTau181 data, N(%)		92 (29)	59 (50)†	34 (45)	30 (43)	-	-
pTau181 Status, N(%)	-	75 (82)	27 (46)†	22 (65)	6 (20)†	75 (82)	27 (46)†
	+	17 (18)	32 (54)	12 (35)	24 (80)	17 (18)	32 (54)
APOE ε4, N(%)	-	242 (84)	74 (71)*	56 (85)	41 (63)*	69 (81)	36 (72)
	+	47 (16)	30 (19)	10 (15)	24 (37)	16 (19)	14 (28)
Cognitive Assessment and Brain Structure, mean ± SD							
MMSE		28.3 ± 1.7	23.5 ± 4.8†	28.7 ± 1.3	22.5 ± 4.9†	27.9 ± 2.2	23.2 ± 5.1†
LMII		22.6 ± 7.7	7.9 ± 7.6†	21.8 ± 6.6	5.0 ± 6.2†	21.5 ± 6.9	7.5 ± 7.0†
LMI		38.3 ± 10.5	19.2 ± 10.8†	37.1 ± 8.3	15.4 ± 8.9†	36.8 ± 9.0	18.0 ± 9.3†
DS		27.8 ± 5.4	21.3 ± 5.8†	26.7 ± 5.7	20.8 ± 5.4†	27.3 ± 5.8	20.6 ± 5.4†
DSST		65.4 ± 17.0	40.5 ± 17.5†	62.2 ± 15.9	36.4 ± 16.3†	62.8 ± 17.4	42.3 ± 18.4†
CTT1		51.8 ± 22.6	103.9 ± 68.1†	54.8 ± 23.0	118.4 ± 71.2†	55.2 ± 27.3	101.5 ± 68.0†
CTT2		112.1 ± 41.9	204.5 ± 89.7†	120.7 ± 44.3	216.9 ± 90.9†	114.3 ± 46.4	204.0 ± 94.7†
SCWT-word		97.6 ± 18.7	74.4 ± 23.2†	94.6 ± 21.2	69.4 ± 22.7†	93.5 ± 18.1	76.2 ± 24.3†
SCWT-color		79.4 ± 16.3	56.3 ± 17.6†	78.7 ± 16.7	55.3 ± 18.3†	77.8 ± 16.5	54.4 ± 16.2†
SCWT-colored word		40.4 ± 13.8	22.0 ± 14.5†	40.2 ± 15.0	22.2 ± 16.6†	39.5 ± 12.8	22.4 ± 11.4†
SCWT-interference		-3.4 ± 10.3	-10.0 ± 12.9†	-3.0 ± 11.0	-8.6 ± 14.1*	-3.2 ± 8.5	-9.4 ± 10.4†
VF		37.1 ± 7.8	24.8 ± 8.5†	38.3 ± 9.4	22.9 ± 8.6†	38.3 ± 7.5	25.3 ± 8.0†
BNT		25.0 ± 2.8	20.5 ± 5.0†	25.0 ± 2.6	20.0 ± 5.2†	24.8 ± 2.7	21.0 ± 4.5†
Memory		0.39 ± 0.77	-1.07 ± 0.76†	0.31 ± 0.65	-1.36 ± 0.62†	0.28 ± 0.68	-1.12 ± 0.70†
Attention		0.32 ± 0.56	-0.90 ± 0.83†	0.20 ± 0.53	-1.12 ± 0.79†	0.22 ± 0.57	-0.91 ± 0.78†
Executive		0.28 ± 0.49	-0.78 ± 0.72†	0.29 ± 0.52	-0.87 ± 0.82†	0.31 ± 0.45	-0.74 ± 0.69†
Language		0.29 ± 0.69	-0.80 ± 1.25†	0.32 ± 0.66	-0.93 ± 1.28†	0.24 ± 0.67	-0.69 ± 1.12†
Total Brain		1065.3 ± 97.7	1009.7 ± 92.0†	1060.7 ± 108.8	1000.7 ± 89.1†	1068.1 ± 95.1	1015.4 ± 89.9*
Ventricle		28.2 ± 12.8	40.2 ± 18.5†	31.4 ± 12.0	44.0 ± 19.8†	28.9 ± 11.7	39.3 ± 20.2†
Gray Matter		593.6 ± 48.8	563.6 ± 48.5†	591.7 ± 51.7	556.6 ± 45.8†	594.4 ± 46.7	565.9 ± 47.1†
White Matter		445.1 ± 53.4	421.9 ± 50.8†	442.6 ± 59.8	419.7 ± 54.0*	446.6 ± 52.1	424.3 ± 48.2*
Hippocampus		8.1 ± 0.9	7.2 ± 1.1†	7.9 ± 0.8	6.8 ± 1.1†	8.1 ± 0.9	7.3 ± 1.2†
Entorhinal		3.7 ± 0.6	3.2 ± 0.9†	3.7 ± 0.6	3.0 ± 1.0†	3.7 ± 0.6	3.3 ± 0.9†
Amygdala		3.1 ± 0.4	2.7 ± 0.5†	3.1 ± 0.4	2.6 ± 0.4†	3.2 ± 0.4	2.8 ± 0.5†

Table 1 (continued)

	Whole sample		Amyloid subgroup		pTau subgroup	
Characteristics	**Normal**	**MCI**	**Normal**	**MCI**	**Normal**	**MCI**
	***N*=320**	***N*=119**	***N*=75**	***N*=70**	***N*=92**	***N*=59**
AD-CTS	2.52±0.10	2.46±0.12†	2.52±0.09	2.43±0.11†	2.52±0.09	2.49±0.10
CC	0.62±0.03	0.59±0.05†	0.62±0.03	0.57±0.04†	0.62±0.03	0.59±0.05†
FX	0.42±0.09	0.34±0.10†	0.39±0.09	0.32±0.10†	0.41±0.09	0.35±0.10†
TP	0.44±0.04	0.40±0.05†	0.43±0.03	0.39±0.05†	0.43±0.04	0.41±0.05†
FMA	0.60±0.03	0.58±0.04†	0.60±0.03	0.57±0.04†	0.60±0.03	0.58±0.04*
CST	0.62±0.02	0.61±0.03†	0.62±0.02	0.60±0.03†	0.62±0.02	0.61±0.03*
CR	0.47±0.03	0.45±0.03†	0.46±0.03	0.44±0.03†	0.46±0.03	0.45±0.03*
ATR	0.40±0.03	0.37±0.03†	0.39±0.02	0.36±0.03†	0.40±0.03	0.38±0.03†
PTR	0.54±0.03	0.52±0.03†	0.54±0.03	0.51±0.03†	0.54±0.03	0.53±0.03
IC	0.62±0.02	0.60±0.03†	0.61±0.02	0.60±0.03†	0.61±0.02	0.60±0.03*
EC	0.37±0.02	0.36±0.03†	0.37±0.02	0.35±0.02	0.37±0.02	0.36±0.03*
CCG	0.51±0.04	0.48±0.05†	0.50±0.03	0.46±0.04	0.51±0.03	0.48±0.04†
CGH	0.36±0.03	0.34±0.04†	0.35±0.04	0.33±0.04	0.35±0.03	0.34±0.03
SLF	0.42±0.02	0.41±0.03†	0.42±0.02	0.41±0.03	0.42±0.02	0.41±0.03*
ILF	0.46±0.02	0.44±0.03†	0.45±0.02	0.44±0.02	0.45±0.02	0.45±0.03
SFOF	0.46±0.04	0.42±0.05†	0.45±0.04	0.41±0.05	0.46±0.04	0.43±0.05†
IFOF	0.44±0.02	0.42±0.03†	0.44±0.02	0.41±0.03	0.44±0.02	0.43±0.03*
UF	0.41±0.02	0.39±0.03†	0.41±0.02	0.38±0.03	0.41±0.02	0.40±0.03*
AD-WMIS	0.48±0.02	0.45±0.03†	0.47±0.02	0.44±0.03	0.48±0.02	0.46±0.03†

BMI, body max index; MMSE, Mini-Mental State Examination; LM, Logical Memory Test; DS, Digit Span; DSST, Digit Symbol Substitute Test; CTT, Color Trails Test; VF, Semantic Verbal Fluency; SCWT, Stroop Color and Word Test; BNT, Boston Naming Test; AD-CTS, AD cortical thickness score; CC, Corpus Callosum; FX, Fornix; TP, Tapetum; FMA, Forceps Major; CST, Corticospinal Tract; CR, Corona Radiata; ATR, Anterior Thalamic Radiation; PTR, Posterior Thalamic Radiation; IC, Internal Capsule; EC, External Capsule; CCG, Cingulum Cingulate Gyrus; CGH, Cingulum Hippocampus; SLF, Superior Longitudinal Fasciculus; ILF, Inferior Longitudinal Fasciculus; SFOF, Superior Fronto-occipital Fasciculus; IFOF, Inferior Fronto-occipital Fasciculus; UF, Uncinate Fasciculus; AD-WMIS, AD white matter integrity score

* p-value < 0.05

† p-value < 0.001

‡ Vegetarian, a person who does not eat meat or meat products; Flexitarian, a person who follows a vegetarian diet but occasionally eats meat or fish; Non-vegetarian, a person who eats meat

§ Never, less than 1 time per week; Sometimes, more than 1 but less than 5 times per week; Frequently, more than 5 times per week

terms partially contributed by these key microbes. In this exploratory analysis, approximately 16,000 mediation tests were performed, as detailed in Supplementary Table S11. Of these, 60 significant mediation relationships were identified and are summarized in Table 3. The most prominent bacterial functions identified involved proteins participating in DNA and RNA metabolism, NAD redox reactions, and energy generation, highlighting their potential relevance to cognitive and neuroimaging outcomes.

Co-occurrence network of key microbes

The co-occurrence networks of 59 key microbes were analyzed using three algorithms: SPIEC-EASI (Fig. 2), SPRING, and gCoda (Supplementary Fig. S5). Across these networks, *Enterocloster bolteae*, a species positively associated with pTau levels, emerged as a central hub among the key microbes. This species exhibited synergistic interactions with other pathogens, including *Clostridium symbiosum*, *Bacteroides thetaiotaomicron*, *Flavonifractor plautii*, and *Faecalimonas umbilicata*. Additionally, *Enterocloster bolteae* appeared to compete with and inhibit the co-occurrence of beneficial microbes. In the SPIEC-EASI network, there are four clusters. Among them, *Streptococcus* species demonstrated strong co-occurrence with one another and were independent from the other three clusters, suggesting possible mutual reinforcement of their effects. These findings highlight the intricate interplay between pathogenic and beneficial microbes within the microbial community and their potential roles in cognitive impairment.

Discussion

This study, leveraging a well-defined cohort, revealed notable compositional and functional changes in the gut microbiota of individuals with cognitive impairment. Fifty-nine key microbial species were identified, showing associations with MCI, AD pathology—including amyloid PET and pTau181—and the APOE-ε4 risk allele. These findings were validated through analyses linking these microbes to neuroimaging metrics (T1-weighted and DTI imaging) and cognitive performance. Furthermore, we explored the interactions among these microbial species and their involvement in metabolic pathways,

Table 2 Key microbes discovered by differential abundance analysis

Species	MCI	A + MCI	T + MCI	A + T +	APOE4 +
Adlercreutzia equolifaciens	-				
Alistipes communis	-				
Bacteroides eggerthii	-			-	-
Bacteroides intestinalis	-			-	
Bacteroides thetaiotaomicron	+		+		
Bifidobacterium dentium	+				
Bifidobacterium pseudocatenulatum	-				
Clostridiaceae bacterium	-			-	
Clostridium scindens	+				
Clostridium symbiosum	+			+	
Dialister hominis	-			-	
Eisenbergiella tayi	+				
Enterococcus faecium	-				
Fusicatenibacter saccharivorans	-		-		
Lacrimispora amygdalina	-				
Parasutterella excrementihominis	-				
Phocaeicola dorei	-				
Prevotella copri clade C	+				
Roseburia faecis	-	-			
Ruminococcus lactaris	-		-		
Ruminococcus torques	+				
Streptococcus anginosus	+				
Akkermansia muciniphila		-		-	
Anaerobutyricum soehngenii		+			
Blautia glucerasea		-	-	-	
Butyricimonas virosa		+			
Holdemanella biformis		+			
Lachnospiraceae bacterium		-			
Neobittarella massiliensis		+		+	
Parabacteroides merdae		+	+		
Anaerostipes hadrus			-		
Bacteroides salyersiae			-		
Blautia obeum			-	-	
Dialister invisus			-		
Enterocloster bolteae			+		
Hungatella hathewayi			+		+
Klebsiella variicola			+		
Lachnospira eligens			-		
Romboutsia timonensis			-		
Ruminococcus bromii			-		-
Anaerotruncus rubiinfantis				-	
Barnesiella intestinihominis				-	
Blautia faecis				-	
Blautia luti				-	
Dorea formicigenerans				-	
Faecalimonas umbilicata				+	
Flavonifractor plautii				+	
Fusobacterium mortiferum				+	
Fusobacterium varium				+	
Intestinimonas butyriciproducens				-	
Streptococcus australis				-	
Streptococcus salivarius				-	
Waltera intestinalis				-	

Table 2 (continued)

Species	MCI	A + MCI	T + MCI	A + T +	APOE4 +
Allisonella histaminiformans					-
Anaerotruncus colihominis					-
Bacteroides clarus					+
Holdemanella porci					-
Streptococcus cristatus					+
Streptococcus mitis					+

[+], positive association; [−], negative association

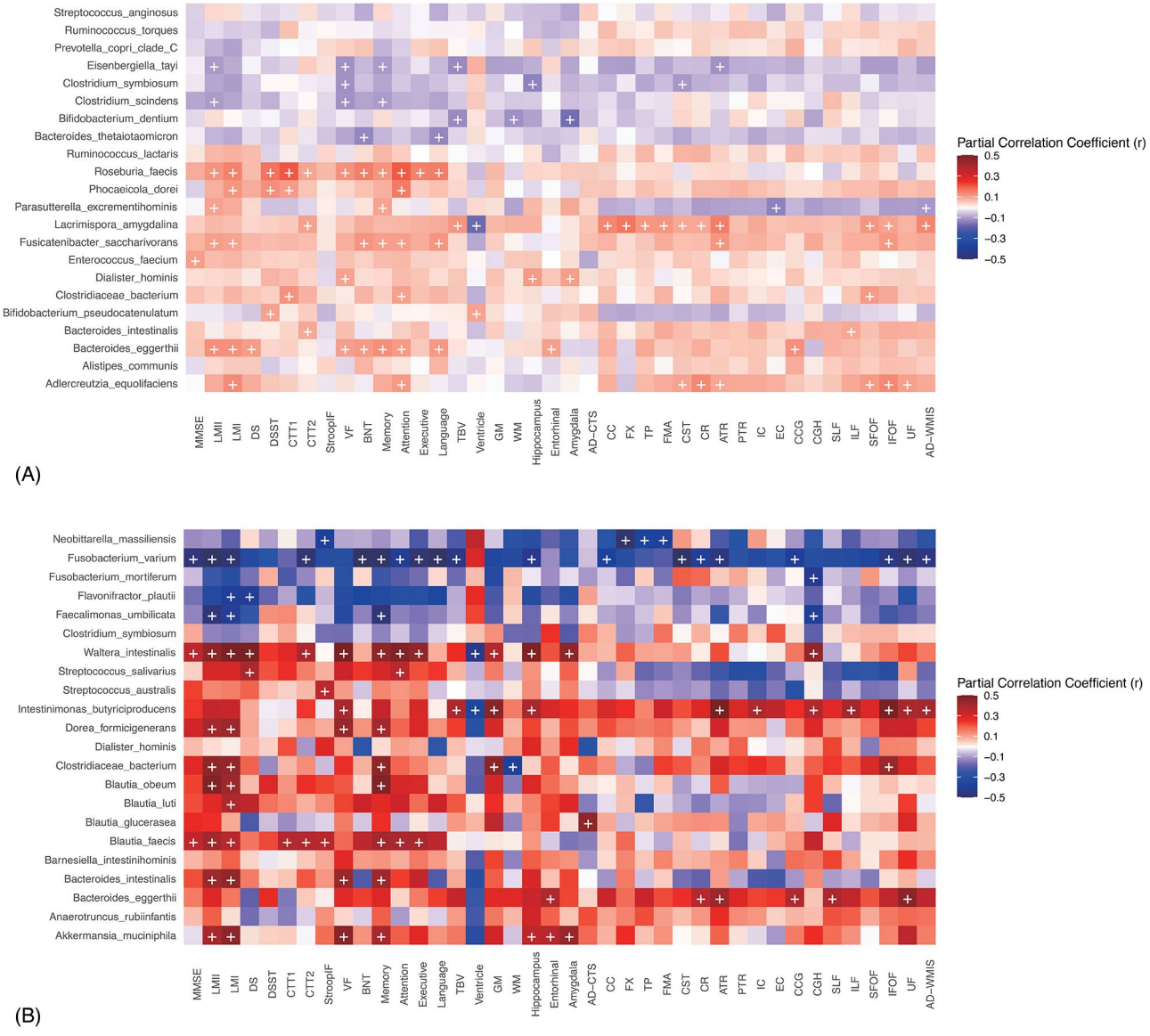

Fig. 1 Correlation Heatmaps of Key Microbes and Cognitive Functions/Brain Structure in (**A**) Whole Dataset and (**B**) AT subgroup. Partial correlations between key microbial species and neuropsychological test scores were adjusted for age, gender, and years of education. For consistency in interpretation, the outcomes of Color Trails Test 1 and 2 were assigned a negative sign so that the correlation colors would reflect the same direction across measures. Partial correlations between key microbial species and brain volume indicators, as well as fractional anisotropy (FA) from DTI analysis, were adjusted for age, gender, and estimated intracranial volume (eTIV). Correlations between key microbial species and the AD-CTS, a cortical thickness indicator, were adjusted only for age and gender. The cross sign indicates a significant correlation with $p < 0.05$. Key microbes that show correlations with a greater number of cognitive functions and brain structures are considered more robust in their relationship with cognitive impairment

Table 3 Significant mediations of KEGG ontology between key microbes and cognitive functions/brain structure

Sub-group	Species	Cognitive functions/ Brain structure	Mediator KO	ACME	*P*	ADE	*P*	TE	*P*
all	*Roseburia faecis*	Language	K09702: hypothetical protein	0.004	0.004	0.037	0.004	0.041	0.000
all	*Clostridium symbiosum*	Hippocampus	K01997: branched-chain amino acid transport system permease protein	-0.006	0.026	-0.025	0.036	-0.031	0.014
all	*Bacteroides thetaiotaomicron*	Language	K09469: 2-aminoethylphosphonate-pyruvate transaminase	-0.038	0.002	-0.012	0.604	-0.051	0.036
all	*Fusicatenibacter saccharivorans*	Language	K02030: polar amino acid transport system substrate-binding protein	-0.005	0.014	0.041	0.008	0.036	0.024
all	*Fusicatenibacter saccharivorans*	Language	K03826: putative acetyltransferase	0.003	0.028	0.032	0.020	0.035	0.008
all	*Adlercreutzia equolifaciens*	Attention	K08600: sortase B	-0.004	0.022	0.025	0.000	0.021	0.008
all	*Bifidobacterium dentium*	TBV	K02037: phosphate transport system permease protein	-0.453	0.030	-1.347	0.082	-1.800	0.026
all	*Bifidobacterium dentium*	TBV	K02346: DNA polymerase IV	-0.290	0.044	-1.494	0.054	-1.784	0.022
all	*Bifidobacterium dentium*	TBV	K02864: large subunit ribosomal protein L10	-0.416	0.044	-1.350	0.088	-1.766	0.028
all	*Bifidobacterium dentium*	TBV	K03101: signal peptidase II	-0.304	0.040	-1.501	0.048	-1.805	0.020
all	*Bifidobacterium dentium*	TBV	K03980: putative peptidoglycan lipid II flippase	-0.304	0.012	-1.485	0.056	-1.788	0.018
all	*Bifidobacterium dentium*	TBV	K05799: GntR family transcriptional regulator, transcriptional repressor for pyruvate dehydrogenase complex	-0.301	0.040	-1.489	0.044	-1.790	0.018
all	*Bifidobacterium dentium*	TBV	K13788: phosphate acetyltransferase	-0.382	0.036	-1.396	0.066	-1.778	0.024
all	*Bacteroides eggerthii*	Language	K01142: exodeoxyribonuclease III	0.006	0.018	0.019	0.116	0.025	0.026
all	*Fusicatenibacter saccharivorans*	Attention	K00077: 2-dehydropantoate 2-reductase	-0.006	0.026	0.028	0.018	0.023	0.042
all	*Fusicatenibacter saccharivorans*	Attention	K03465: thymidylate synthase (FAD)	-0.008	0.038	0.031	0.008	0.023	0.032
all	*Bifidobacterium dentium*	WM	K02346: DNA polymerase IV	-0.259	0.022	-0.974	0.098	-1.232	0.028
all	*Bifidobacterium dentium*	WM	K03980: putative peptidoglycan lipid II flippase	-0.209	0.018	-1.027	0.068	-1.235	0.026
all	*Bifidobacterium dentium*	WM	K16147: starch synthase (maltosyl-transferring)	-0.375	0.008	-0.866	0.188	-1.241	0.030
all	*Bifidobacterium dentium*	WM	K16784: biotin transport system ATP-binding protein	-0.498	0.014	-0.721	0.256	-1.220	0.046
all	*Bacteroides eggerthii*	Entorhinal	K03169: DNA topoisomerase III	-0.004	0.024	0.022	0.012	0.018	0.040
all	*Bifidobacterium pseudocatenulatum*	Ventricle	K00528: ferredoxin–NADP + reductase	0.052	0.048	0.286	0.098	0.338	0.044
all	*Bifidobacterium pseudocatenulatum*	Ventricle	K03723: transcription-repair coupling factor (superfamily II helicase)	0.068	0.020	0.257	0.134	0.325	0.038
all	*Bifidobacterium pseudocatenulatum*	Ventricle	K04092: chorismate mutase	0.108	0.014	0.223	0.202	0.330	0.042
A	*Parabacteroides merdae*	Hippocampus	K00651: homoserine O-succinyltransferase	0.013	0.034	-0.084	0.004	-0.071	0.010
A	*Parabacteroides merdae*	Hippocampus	K02876: large subunit ribosomal protein L15	0.012	0.042	-0.083	0.002	-0.070	0.010
A	*Parabacteroides merdae*	Hippocampus	K03664: SsrA-binding protein	0.013	0.034	-0.084	0.004	-0.071	0.012
A	*Parabacteroides merdae*	TBV	K03664: SsrA-binding protein	0.450	0.044	-3.392	0.002	-2.942	0.016
A	*Fusicatenibacter saccharivorans*	Memory	K20490: lantibiotic transport system ATP-binding protein	0.017	0.034	0.057	0.118	0.074	0.036
AT	*Fusobacterium varium*	Memory	K03826: putative acetyltransferase	-0.029	0.048	-0.181	0.012	-0.211	0.004
AT	*Blautia obeum*	Memory	K03575: A/G-specific adenine glycosylase	-0.035	0.036	0.187	0.000	0.152	0.002
AT	*Blautia obeum*	Memory	K06023: HPr kinase/phosphorylase	0.044	0.022	0.106	0.040	0.150	0.006
AT	*Intestinimonas butyriciproducens*	GM	K02992: small subunit ribosomal protein S7	-1.030	0.046	4.808	0.000	3.777	0.024

Table 3 (continued)

Sub-group	Species	Cognitive functions/ Brain structure	Mediator KO	ACME	*P*	ADE	*P*	TE	*P*
AT	*Intestinimonas butyriciproducens*	GM	K18331: NADP-reducing hydrogenase subunit HndC	-2.206	0.032	5.894	0.000	3.688	0.044
AT	*Bacteroides intestinalis*	Memory	K02952: small subunit ribosomal protein S13	-0.039	0.036	0.157	0.000	0.119	0.006
AT	*Bacteroides intestinalis*	Memory	K06989: aspartate dehydrogenase	-0.113	0.006	0.231	0.000	0.119	0.004
AT	*Akkermansia muciniphila*	Memory	K01515: ADP-ribose pyrophosphatase	0.038	0.048	0.068	0.072	0.105	0.002
AT	*Intestinimonas butyriciproducens*	AD-WMIS	K02992: small subunit ribosomal protein S7	-0.001	0.046	0.004	0.002	0.003	0.018
AT	*Intestinimonas butyriciproducens*	TBV	K18331: NADP-reducing hydrogenase subunit HndC	-2.937	0.028	7.755	0.000	4.818	0.042
APOE	*Streptococcus mitis*	Attention	K01819: galactose-6-phosphate isomerase	-0.005	0.020	0.044	0.002	0.039	0.008
APOE	*Streptococcus mitis*	Attention	K01883: cysteinyl-tRNA synthetase	-0.008	0.026	0.046	0.000	0.038	0.006
APOE	*Streptococcus mitis*	Attention	K02835: peptide chain release factor RF-1	-0.006	0.030	0.044	0.008	0.039	0.010
APOE	*Streptococcus mitis*	Attention	K02950: small subunit ribosomal protein S12	-0.013	0.044	0.051	0.002	0.038	0.006
APOE	*Streptococcus cristatus*	Hippocampus	K00674: 2,3,4,5-tetrahydropyridine-2-carboxylate N-succinyltransferase	-0.015	0.018	0.079	0.008	0.064	0.024
APOE	*Streptococcus cristatus*	Hippocampus	K00872: homoserine kinase	-0.021	0.020	0.084	0.000	0.063	0.028
APOE	*Streptococcus cristatus*	Hippocampus	K01756: adenylosuccinate lyase	-0.016	0.042	0.079	0.004	0.063	0.030
APOE	*Streptococcus cristatus*	Hippocampus	K01878: glycyl-tRNA synthetase alpha chain	-0.018	0.016	0.082	0.012	0.064	0.030
APOE	*Streptococcus cristatus*	Hippocampus	K01879: glycyl-tRNA synthetase beta chain	-0.025	0.004	0.088	0.004	0.063	0.026
APOE	*Streptococcus cristatus*	Hippocampus	K01916: NAD + synthase	-0.017	0.022	0.083	0.008	0.066	0.020
APOE	*Streptococcus cristatus*	Hippocampus	K02244: comGB; competence protein ComGB	-0.015	0.026	0.079	0.002	0.064	0.006
APOE	*Streptococcus cristatus*	Hippocampus	K03621: phosphate acyltransferase	-0.019	0.012	0.086	0.002	0.067	0.018
APOE	*Streptococcus cristatus*	Hippocampus	K03706: transcriptional pleiotropic repressor	-0.012	0.046	0.076	0.010	0.064	0.018
APOE	*Streptococcus cristatus*	Hippocampus	K03784: purine-nucleoside phosphorylase	-0.015	0.048	0.080	0.000	0.064	0.024
APOE	*Streptococcus cristatus*	Hippocampus	K05823: N-acetyldiaminopimelate deacetylase	-0.016	0.032	0.082	0.006	0.066	0.006
APOE	*Streptococcus cristatus*	Hippocampus	K07146: UPF0176 protein	-0.019	0.026	0.084	0.006	0.065	0.022
APOE	*Streptococcus cristatus*	Hippocampus	K10563: formamidopyrimidine-DNA glycosylase	-0.014	0.030	0.078	0.006	0.064	0.016
APOE	*Streptococcus cristatus*	Hippocampus	K21064: 5-amino-6-(5-phospho-D-ribityl-amino)uracil phosphatase	-0.015	0.026	0.078	0.002	0.063	0.018
APOE	*Streptococcus cristatus*	Hippocampus	K21567: ferredoxin/ flavodoxin—NADP + reductase	-0.015	0.024	0.080	0.000	0.065	0.008
APOE	*Anaerotruncus colihominis*	Ventricle	K03205: type IV secretion system protein VirD4	-0.172	0.012	0.818	0.018	0.646	0.044
APOE	*Allisonella histaminiformans*	TBV	K03704: cold shock protein (beta-ribbon, CspA family)	0.424	0.016	-2.198	0.004	-1.774	0.046

all, whole sample; A, A + MCI versus A - MCI; AT, A + T + versus A - T -; APOE, APOE4 + versus APOE4 -

offering insights into their potential roles in cognitive decline and neurodegenerative processes.

As highlighted in previous 16 S rRNA studies [40], the finding that no significant differences in gut microbiota biodiversity were observed between individuals with MCI and those with normal cognition aligns with earlier research. However, reported differences in microbial composition and function between MCI patients and healthy controls have shown considerable variability across studies. Discrepancies between studies likely stem from experimental differences, including variations in participant selection, diagnostic criteria, nucleic acid preparation, and sequencing protocols. Computational factors, such as algorithm choice and reference databases, also significantly influence results [41, 42]. These methodological and computational challenges complicate

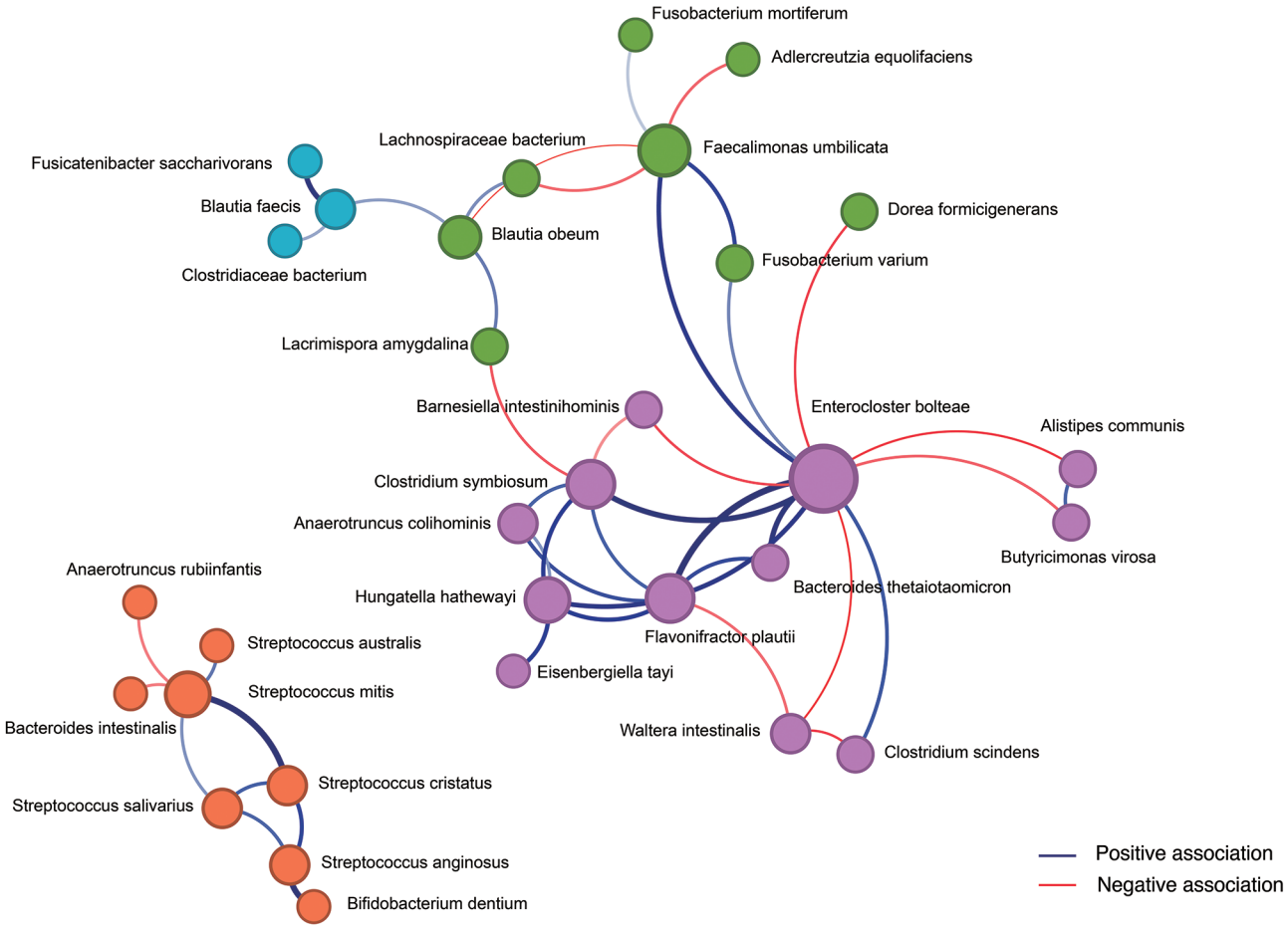

Fig. 2 Co-occurrence Network Analysis of Key Microbes with SPIEC-EASI. The color of the nodes represents the clusters of each key microbial species, with blue edges indicating positive associations between species and red edges indicating negative associations. The intensity of the edge color corresponds to the strength of the association. Larger nodes indicate a higher degree of connectivity, and *Enterocloster bolteae* was identified as the central hub in this co-occurrence network.

comparisons across microbiome studies and hinder the generalizability of findings.

Previous 16S rRNA studies involving both MCI and AD patients have reported progressive shifts in gut microbiome composition from normal cognition to MCI and subsequently to AD. Genera such as *Ruminococcus*, *Blautia*, and *Lachnospira* were consistently more abundant in cognitively normal individuals compared to those with MCI or AD. In contrast, *Bacteroides*, *Escherichia*, and *Prevotella* were more prevalent in individuals across the AD spectrum and are considered potentially pathogenic [43–45]. Using shotgun metagenomic sequencing, Jia et al. demonstrated that microbial alterations from normal cognition through slight cognitive symptoms, subtle cognitive decline, MCI, and AD generally follow a consistent directional trend. Stage-specific taxa, particularly species within *Alistipes*, *Bacteroides*, and *Prevotella*, may contribute to AD pathogenesis via mechanisms involving neuroinflammation and neurotransmitter dysregulation. Conversely, *Streptococcus* species may confer protective effects by modulating anti-inflammatory responses [46]. These microbial patterns are largely consistent with those observed in our study.

Few studies have utilized shotgun metagenomic sequencing to explore gut microbiota in MCI/AD or the context of cognitive impairment, resulting in a lack of sufficient evidence to directly compare our findings, particularly concerning the read depth necessary for microbial species identification. Additionally, research investigating the associations between specific microbial species and AD pathology remains limited. Ma et al. conducted a substudy involving 515 participants to investigate the role of the gut microbiome in the relationship between bowel movement frequency and cognitive functions. They identified 15 species significantly associated with cognitive function, including *Bacteroides thetaiotaomicron* and *Clostridium symbiosum*, which were also linked to poorer cognitive functions in our study [47]. Dilmore et al. examined the effects of a ketogenic diet in 11 cognitively normal individuals and 9 MCI patients,

reporting increased levels of *Dialister* and *Bacteroides* in cognitively normal participants [48]. Their findings suggest that a high-fat modified Mediterranean ketogenic diet may benefit adults with MCI by enriching *Akkermansia muciniphila* and modulating GABA-regulating microbes, potentially enhancing cognitive outcomes. Consistent with their findings, we also observed that these taxa were enriched in individuals with better cognitive status.

Two observational studies closely align with our study design and findings. Ferreiro et al. investigated the taxonomic composition and gut microbial function in 49 preclinical AD participants and 115 healthy controls in the USA. Preclinical AD was defined as a Clinical Dementia Rating (CDR) of 0 combined Aβ positivity, determined by PET imaging or CSF Aβ42/Aβ40 ratio [11]. They identified several species, including *Bacteroides intestinalis*, *Dorea formicigenerans*, *Blautia obeum*, *Barnesiella intestinihominis*, *Anaerostipes hadrus*, and *Ruminococcus lactaris*, which were more abundant in the preclinical AD group. Interestingly, in our study, these species were associated with normal cognitive status and biomarkers. Ferreiro et al. primarily aimed to leverage gut microbiome signatures for improving early screening measures for AD risk. Li et al. conducted a study involving 33 dementia patients, 125 MCI patients, and 358 cognitively normal participants in China [12]. Their findings align with ours in several significant ways. Consistent with our results, they found no significant differences in biodiversity indices. Differential taxonomic profiles included *Holdemanella biformis*, *Fusicatenibacter saccharivorans*, *Clostridium symbiosum*, *Bifidobacterium pseudocatenulatum*, and *Anaerostipes hadrus*, all of which exhibited the same direction of association in our study. This further underscores the consistency of findings across diverse populations and supports the relevance of these species in the context of cognitive health.

In our study, we identified 59 species associated with cognitive impairment and AD etiology, including *A. muciniphila*, a next-generation probiotic with therapeutic potential for enhancing brain function [49]. It reduces anxiety-like behaviors, lowers pro-inflammatory cytokines, and enhances spatial and recognition memory in tau protein-induced rat models [50]. Additionally, it reduced Aβ40–42 levels in the cerebral cortex of APP/PS1 mice and improved their Y-maze test performance [51]. Higarza et al. further demonstrated its role in boosting brain oxidative metabolism by restoring mitochondrial cytochrome C oxidase activity, supporting *A. muciniphila*'s role in energy production of brain [52]. However, despite its reputation as a beneficial probiotic, emerging evidence highlights its context-dependent effects. *A. muciniphila* has been shown to increase in Parkinson's disease, possibly by inducing mitochondrial calcium overload in enteroendocrine cells, leading to reactive oxygen species generation and following α-synuclein aggregation [53]. Additionally, it may promote colorectal cancer progression by upregulating proliferation-related genes and exacerbating inflammation [54]. These findings underscore the still unclear and controversial nature of *A. muciniphila* as a therapeutic target.

Our findings showed a positive mediation effect involving *A. muciniphila*, ADP-ribose pyrophosphatase, and memory performance. ADP-ribose pyrophosphatase catalyzes the hydrolysis of ADP-ribose into AMP and ribose-5-phosphate, playing a crucial role in NAD + metabolism. As a key metabolic intermediate, ADP-ribose is involved in neuronal energy homeostasis and oxidative stress regulation [55]. However, excessive ADP-ribose can activate poly-ADP-ribose polymerase (PARP), leading to NAD + depletion and subsequent neuronal death. Accumulation of poly(ADP-ribose) has been implicated in α-synuclein-mediated neurodegeneration in Parkinson's disease [56] and the progression of AD [57, 58]. These findings imply that *A. muciniphila* may modulate NAD+-related pathways, potentially influencing cognitive resilience and neurodegeneration. Beyond *A. muciniphila*, other beneficial microbes identified in our study were aligned with previous studies. *Phocaeicola dorei* was significantly and negatively correlated with AD Assessment Scale-Cognitive Subscale (ADAS-Cog) scores [59]. *Intestinimonas butyriciproducens*, linked to autism [60], converts lysine into butyrate, an energy source for colonocytes, with known anti-carcinogenic, anti-inflammatory, and anti-oxidative effects [61]. Other genera consistent with the key microbes identified in our study—*Blautia*, *Ruminococcus*, and *Roseburia*—also demonstrated reductions in AD participants in previous studies and are known to possess potential probiotic properties [43, 62, 63].

In contrast, some key microbes have been implicated in pathogenic effects on cognitive functions. Previous reports on the effects of genus *Bacteroides* were conflicting. Our results indicated that different species of the genus Bacteroides have opposite effects on MCI risk. Particularly, *Bacteroides thetaiotaomicron*, which is a major bacteria species responsible for breaking down complex polysaccharides, is increased in MCI and T + individuals. While *B. thetaiotaomicron* has been reported to exhibit anti-inflammatory effects and be beneficial in colitis, another recent report also found an increase in *B. thetaiotaomicron* in MCI individuals [64]. Abraham et al. reported that elevated levels of *B. thetaiotaomicron* were associated with poorer performance in the Morris Maze Test, and this bacterial group was significantly more abundant in the microbiome of APP/PS1TG mice compared to wild-type controls [65]. Similarly, Zha et al.

treated 5xFAD mice with five *Bacteroides* strains, including *B. thetaiotaomicron*. While most *Bacteroides* strains significantly reduced Aβ plaque formation in the hippocampal regions, this effect was not observed in mice treated with *B. thetaiotaomicron* or *B. caccae*, highlighting a unique characteristic of *B. thetaiotaomicron* within the genus [66]. Other microbes have also shown pathogenic potential. *Enterocloster bolteae* is a bacterium frequently identified in the gut microbiome of children with autism spectrum disorder and produces metabolites suspected to have neurotoxic effects [67]. *Butyricimonas virosa*, though rare, has been associated with bacteremia in certain patients [68]. Additionally, increased levels of *Parabacteroides* species were observed in rats following high sugar consumption during adolescence. This led to altered gene expression in pathways related to intracellular kinase activity and synaptic neurotransmitter signaling, ultimately impairing hippocampal function [69].

Our results also found that *Clostridum* species are associated with risk for MCI. *Clostridium Scindens* and *Clostridium Symbiosum* are both important bacteria species capable of converting primary bile acid to secondary bile acid compounds, such as deoxycholic acid [70]. Emerging evidence, including our unpublished data, suggests that deoxycholic acid levels are elevated in patients with MCI and dementia [71, 72]. This increase is likely mediated by the relative enrichment of these bacterial species in the gut microbiota of individuals with MCI. In our analysis, *C. symbiosum* has been identified as a key microbe linked to branched-chain amino acid (BCAA) metabolism and hippocampal volume. BCAAs—leucine, isoleucine, and valine—play a crucial role in brain function, influencing neurotransmitter synthesis and neural signaling. They share transport mechanisms across the blood-brain barrier with large neutral amino acids (LNAAs), including dopamine, serotonin, and norepinephrine precursors [73, 74]. BCAA supplementation has also been shown to support cognitive recovery following traumatic brain injury by restoring neurotransmitter levels and promoting neural repair [75]. Recent studies have explored BCAAs' role in neurodegenerative diseases such as AD [76] and PD. A 2018 prospective study across eight cohorts found that higher circulating BCAA levels were associated with a lower risk of AD, implying a neuroprotective effect [77]. Additionally, gut microbiota contributes to BCAA biosynthesis, with shifts in microbial composition linked to fluctuations in BCAA levels in PD [78]. Dietary interventions targeting gut microbiota have emerged as a potential alternative source of BCAAs for individuals at risk of AD [79].

Our research had several notable strengths. First, the study population was drawn from a well-characterized community-based cohort with an adequate sample size, ensuring broad representation and statistical robustness. Additionally, the diagnosis of MCI was rigorously established through a consensus panel of experts, enhancing diagnostic accuracy. Second, we utilized a state-of-the-art pipeline for shotgun metagenomic sequencing, known for its superior sensitivity combined with an up-to-date reference database. Third, we employed rigorous analytical methods to identify key microbial species, corroborating their associations by examining relationships with cognitive functions and neuroimaging metrics, which strengthened the validity of our findings. Furthermore, we explored potential pathways linking gut microbiota to cognitive impairment through mediation analysis and co-occurrence network construction, allowing us to fully leverage our data.

This study is not without limitations. First, relying on a single fecal sample per participant hindered our ability to assess temporal dynamics, as gut microbiota composition is known to vary over time. In addition, the sample size of AD biomarker subgroups was not sufficient to make a robust conclusion. Furthermore, the absence of data on metabolites and pro-inflammatory markers limited our ability to establish definitive mechanistic pathways, leaving our interpretations largely hypothetical. Second, although we carefully adjusted for covariates in our analyses, residual and unmeasured confounding factors may still exist. For example, while educational attainment was included as a covariate in cognitive function analyses, it may not fully capture related factors such as lifestyle behaviors, dietary patterns, or socioeconomic conditions, which can directly or indirectly impact gut microbiota composition.

Conclusions

In summary, we report microbiome compositional and functional alterations in MCI and AD pathology, which further correlate with performance across all cognitive domains and brain structures. Notably, species within the same genus could exert differing impacts on brain health. These findings support the role of gut microbial species in the pathogenesis of cognitive impairment, potentially acting synergistically with traditional AD pathology. Longitudinal follow-up studies incorporating metabolomic and immune profiling, as well as detailed assessments of lifestyle, medication use, and diet, are needed to validate the causal mechanisms to the development of neurodegeneration.

Supplementary Information

The online version contains supplementary material available at https://doi.org/10.1186/s13195-025-01769-9.

Supplementary Material 1

Acknowledgements
We appreciate all participants' contributions to the Taiwan Precision Medicine Initiative on Cognitive Impairment and Dementia cohort (TPMIC) study.

Author contributions
YFC and KCF conceptualized the study framework. KCF, CCL, and YFC designed the methodology. YFC, YLC, and YCL contributed to data collection. KCF conducted data analysis, interpreted the results, and drafted the original manuscript. YFC, YLC, and CCL supervised the study and collaborated with SHK in manuscript review and editing. All authors reviewed and approved the final manuscript.

Funding
This work was supported by the Taiwan National Science and Technology Council, previously the Ministry of Science and Technology, under Grants MOST110-2321-B-418, NSTC113-2321-B-418-003, NSTC113-2321-B-418-005, and NSTC112-2314-BA49-047-MY3; and the Far Eastern Memorial Hospital-National Yang Ming Chiao Tung University Joint Research Program under Grant NYCU-FEMH 112DN11.

Data availability
The non-identifiable metagenomic sequencing data generated in this study have been deposited in the NCBI Sequence Read Archive (SRA) under accession number PRJNA1258384. Other individual-level clinical or identifiable data are available from the corresponding author upon request.

Declarations

Ethics approval and consent to participate
Ethical approval was obtained from the Far Eastern Memorial Hospital Research Ethics Committee (110065-F) and the Institutional Review Board of Cardinal Tien Hospital (CTH-110-2-1-014) in accordance with the Declaration of Helsinki. All participants provided informed consent.

Consent for publication
Not applicable.

Competing interests
The authors declare no competing interests.

Author details
[1]School of Medicine, National Yang Ming Chiao Tung University, 155 Sec. 2, Linong St., Beitou Dist, Taipei City 112304, Taiwan
[2]Institute of Biomedical Informatics, National Yang Ming Chiao Tung University, 155 Sec. 2, Linong St., Beitou Dist, Taipei City 112304, Taiwan
[3]Department of Medical Research, Far Eastern Memorial Hospital, 21 Sec. 2, Nanya S. Rd., Banqiao Dist, New Taipei City 220216, Taiwan
[4]Graduate Program in Biomedical Informatics, Graduate Institute of Medicine, Yuan Ze University, 135 Yuan-Tung Rd., Zhongli Dist, Taoyuan City 32003, Taiwan
[5]Graduate Institute of Clinical Medicine, National Taiwan University, 1 Sec. 4, Roosevelt Rd., Da'an Dist, Taipei City 106319, Taiwan
[6]Department of Neurology, College of Medicine, Hanyang University Guri Hospital, 153 Kyougchun-ro, Guri-si 11923, Gyeonggi-do, Republic of Korea
[7]Department of Translational Medicine, Graduate School of Biomedical Science & Engineering, Hanyang University, 222 Wangsimni-ro, Seongdong-gu, Seoul 04763, Republic of Korea
[8]Department of Neurology, Cardinal Tien Hospital, 362 Zhongzheng Rd., Xindian Dist, New Taipei City 23148, Taiwan
[9]Institute of Public Health, National Yang Ming Chiao Tung University, 155 Sec. 2, Linong St., Beitou Dist, Taipei City 112304, Taiwan
[10]Department of Psychiatry, Far Eastern Memorial Hospital, 21 Sec. 2, Nanya S. Rd., Banqiao Dist, New Taipei City 220216, Taiwan

Received: 18 March 2025 / Accepted: 19 May 2025
Published online: 30 May 2025

References

1. Gauthier S, Reisberg B, Zaudig M, Petersen RC, Ritchie K, Broich K, et al. Mild cognitive impairment. Lancet. 2006;367:1262–70.
2. Jack CR, Bennett DA, Blennow K, Carrillo MC, Dunn B, Haeberlein SB, et al. NIA-AA research framework: toward a biological definition of Alzheimer's disease. Alzheimers Dement. 2018;14:535–62.
3. Karran E, De Strooper B. The amyloid hypothesis in alzheimer disease: new insights from new therapeutics. Nat Rev Drug Discov. 2022;21:306–18.
4. Jack CR Jr, Andrews JS, Beach TG, Buracchio T, Dunn B, Graf A et al. Revised criteria for diagnosis and staging of Alzheimer's disease: Alzheimer's Association Workgroup. Alzheimer's & Dementia. 2024;20:5143–69.
5. Liang Y, Liu C, Cheng M, Geng L, Li J, Du W, et al. The link between gut Microbiome and Alzheimer's disease: from the perspective of new revised criteria for diagnosis and staging of Alzheimer's disease. Alzheimer's Dement. 2024;20:5771.
6. Tarawneh R, Penhos E. The gut Microbiome and Alzheimer's disease: complex and bidirectional interactions. Neurosci Biobehav Rev. 2022;141:104814.
7. Gallo A, Martone AM, Liperoti R, Cipriani MC, Ibba F, Camilli S, et al. Mild cognitive impairment and microbiota: what is known and future perspectives. Front Med (Lausanne). 2024;11:1410246.
8. Jung JH, Kim G, Byun MS, Lee JH, Yi D, Park H, et al. Gut Microbiome alterations in preclinical Alzheimer's disease. PLoS ONE. 2022;17:e0278276.
9. Verhaar BJH, Hendriksen HMA, de Leeuw FA, Doorduijn AS, van Leeuwenstijn M, Teunissen CE, et al. Gut microbiota composition is related to AD pathology. Front Immunol. 2022;12:6030.
10. Vogt NM, Kerby RL, Dill-McFarland KA, Harding SJ, Merluzzi AP, Johnson SC, et al. Gut Microbiome alterations in Alzheimer's disease. Sci Rep. 2017;7:13537.
11. Ferreiro AL, Choi JH, Ryou J, Newcomer EP, Thompson R, Bollinger RM et al. Gut Microbiome composition May be an indicator of preclinical Alzheimer's disease. Sci Transl Med. 2023;15.
12. Li J, Zhu S, Wang Y, Fan M, Dai J, Zhu C, et al. Metagenomic association analysis of cognitive impairment in community-dwelling older adults. Neurobiol Dis. 2023;180:106081.
13. Albert MS, DeKosky ST, Dickson D, Dubois B, Feldman HH, Fox NC, et al. The diagnosis of mild cognitive impairment due to Alzheimer's disease: recommendations from the National Institute on Aging-Alzheimer's association workgroups on diagnostic guidelines for Alzheimer's disease. Alzheimer's Dement. 2011;7:270–9.
14. Martin M. Cutadapt removes adapter sequences from high-throughput sequencing reads. EMBnet J. 2011;17:10–2.
15. Langmead B, Salzberg SL. Fast gapped-read alignment with bowtie 2. Nat Methods. 2012;9:357–9.
16. Blanco-Míguez A, Beghini F, Cumbo F, McIver LJ, Thompson KN, Zolfo M, et al. Extending and improving metagenomic taxonomic profiling with uncharacterized species using metaphlan 4. Nat Biotechnol. 2023;41:1633–44.
17. McMurdie PJ, Holmes S. Phyloseq: an R package for reproducible interactive analysis and graphics of Microbiome census data. PLoS ONE. 2013;8:e61217.
18. Chiu YL, Tsai HH, Lai YJ, Tseng HY, Wu YW, Peng Y, Sen, et al. Cognitive impairment in patients with end-stage renal disease: accelerated brain aging? J Formos Med Assoc. 2019;118:867–75.
19. Fischl B. FreeSurfer Neuroimage. 2012;62:774–81.
20. Dickerson BC, Stoub TR, Shah RC, Sperling RA, Killiany RJ, Albert MS, et al. Alzheimer-signature MRI biomarker predicts AD dementia in cognitively normal adults. Neurology. 2011;76:1395–402.
21. Cui Z, Zhong S, Xu P, He Y, Gong G. PANDA: a pipeline toolbox for analyzing brain diffusion images. Front Hum Neurosci. 2013;7.
22. Mayo CD, Mazerolle EL, Ritchie L, Fisk JD, Gawryluk JR. Longitudinal changes in microstructural white matter metrics in Alzheimer's disease. Neuroimage Clin. 2017;13:330–8.
23. Wen Q, Mustafi SM, Li J, Risacher SL, Tallman E, Brown SA, et al. White matter alterations in early-stage Alzheimer's disease: A tract-specific study. Alzheimer's Dementia: Diagnosis Assess Disease Monit. 2019;11:576–87.
24. Chen Y, Wang Y, Song Z, Fan Y, Gao T, Tang X. Abnormal white matter changes in Alzheimer's disease based on diffusion tensor imaging: A systematic review. Ageing Res Rev. 2023;87:101911.
25. Anderson MJ. Permutational multivariate analysis of variance (PERMANOVA). Wiley StatsRef: Stat Ref Online. 2017. https://doi.org/10.1002/9781118445112.stat07841.
26. Hamidi B, Wallace K, Vasu C, Alekseyenko AV. W D∗ -test: robust distance-based multivariate analysis of variance. Microbiome. 2019;7:1–9.

27. Nearing JT, Douglas GM, Hayes MG, MacDonald J, Desai DK, Allward N, et al. Microbiome differential abundance methods produce different results across 38 datasets. Nat Commun. 2022;13:342.
28. Segata N, Izard J, Waldron L, Gevers D, Miropolsky L, Garrett WS, et al. Metagenomic biomarker discovery and explanation. Genome Biol. 2011;12:R60.
29. Mallick H, Rahnavard A, McIver LJ, Ma S, Zhang Y, Nguyen LH, et al. Multivariable association discovery in population-scale meta-omics studies. PLoS Comput Biol. 2021;17:e1009442.
30. Fernandes AD, Macklaim JM, Linn TG, Reid G, Gloor GB. ANOVA-Like differential expression (ALDEx) analysis for mixed population RNA-Seq. PLoS ONE. 2013;8:e67019.
31. Paulson JN, Colin Stine O, Bravo HC, Pop M. Differential abundance analysis for microbial marker-gene surveys. Nat Methods. 2013;10:1200–2.
32. Tingley D, Yamamoto T, Hirose K, Keele L, Imai K. Mediation: R package for causal mediation analysis. J Stat Softw. 2014;59:1–38.
33. Matchado MS, Lauber M, Reitmeier S, Kacprowski T, Baumbach J, Haller D, et al. Network analysis methods for studying microbial communities: A mini review. Comput Struct Biotechnol J. 2021;19:2687–98.
34. Luo M, Zhu J, Jia J, Zhang H, Zhao J. Progress on network modeling and analysis of gut microecology: a review. Appl Environ Microbiol. 2024;90:e0009224.
35. Liu Z, Ma A, Mathé E, Merling M, Ma Q, Liu B. Network analyses in Microbiome based on high-throughput multi-omics data. Brief Bioinform. 2021;22:1639–55.
36. Peschel S, Müller CL, Von Mutius E, Boulesteix AL, Depner M. NetCoMi: network construction and comparison for Microbiome data in R. Brief Bioinform. 2021;22:bbaa290.
37. Kurtz ZD, Müller CL, Miraldi ER, Littman DR, Blaser MJ, Bonneau RA. Sparse and compositionally robust inference of microbial ecological networks. PLoS Comput Biol. 2015;11:e1004226.
38. Yoon G, Gaynanova I, Müller CL. Microbial networks in SPRING - Semi-parametric rank-based correlation and partial correlation estimation for quantitative microbiome data. Front Genet. 2019;10 JUN:449195.
39. Fang H, Huang C, Zhao H, Deng M. gCoda: conditional dependence network inference for compositional data. J Comput Biol. 2017;24:699–708.
40. Fan K-C, Lin C-C, Liu Y-C, Chao Y-P, Lai Y-J, Chiu Y-L, et al. Altered gut microbiota in older adults with mild cognitive impairment: a case-control study. Front Aging Neurosci. 2023;15:1162057.
41. Bharti R, Grimm DG. Current challenges and best-practice protocols for Microbiome analysis. Brief Bioinform. 2021;22:178–93.
42. McGuinness AJ, Stinson LF, Snelson M, Loughman A, Stringer A, Hannan AJ, et al. From hype to hope: considerations in conducting robust Microbiome science. Brain Behav Immun. 2024;115:120–30.
43. Liu P, Wu L, Peng G, Han Y, Tang R, Ge J, et al. Altered microbiomes distinguish Alzheimer's disease from amnestic mild cognitive impairment and health in a Chinese cohort. Brain Behav Immun. 2019;80:633–43.
44. Li B, He Y, Ma J, Huang P, Du J, Cao L, et al. Mild cognitive impairment has similar alterations as Alzheimer's disease in gut microbiota. Alzheimers Dement. 2019;15:1357–66.
45. Guo M, Peng J, Huang X, Xiao L, Huang F, Zuo Z. Gut Microbiome features of Chinese patients newly diagnosed with Alzheimer's disease or mild cognitive impairment. J Alzheimers Dis. 2021;80:299–310.
46. Jia L, Ke Y, Zhao S, Liu J, Luo X, Cao J, et al. Metagenomic analysis characterizes stage-specific gut microbiota in Alzheimer's disease. Mol Psychiatry. 2025. https://doi.org/10.1038/s41380-025-02973-7.
47. Ma C, Li Y, Mei Z, Yuan C, Kang JH, Grodstein F, et al. Association between bowel movement pattern and cognitive function: prospective cohort study and a metagenomic analysis of the gut Microbiome. Neurology. 2023;101:E2014–25.
48. Dilmore AH, Martino C, Neth BJ, West KA, Zemlin J, Rahman G, et al. Effects of a ketogenic and low-fat diet on the human metabolome, microbiome, and foodome in adults at risk for Alzheimer's disease. Alzheimer's Dement. 2023;19:4805–16.
49. Xu R, Zhang Y, Chen S, Zeng Y, Fu X, Chen T, et al. The role of the probiotic Akkermansia muciniphila in brain functions: insights underpinning therapeutic potential. Crit Rev Microbiol. 2023;49:151–76.
50. Maftoon H, Davar Siadat S, Tarashi S, Soroush E, Basir Asefi M, Rahimi Foroushani A, et al. Ameliorative effects of Akkermansia muciniphila on anxiety-like behavior and cognitive deficits in a rat model of Alzheimer's disease. Brain Res. 2024;1845:149280.
51. Ou Z, Deng L, Lu Z, Wu F, Liu W, Huang D, et al. Protective effects of Akkermansia muciniphila on cognitive deficits and amyloid pathology in a mouse model of Alzheimer's disease. Nutr Diabetes. 2020;10:1–10.
52. Higarza SG, Arboleya S, Arias JL, Gueimonde M, Arias N. Akkermansia muciniphila and environmental enrichment reverse cognitive impairment associated with high-fat high-cholesterol consumption in rats. Gut Microbes. 2021;13:1–20.
53. Amorim Neto DP, Bosque BP, Pereira de Godoy JV, Rodrigues PV, Meneses DD, Tostes K et al. Akkermansia muciniphila induces mitochondrial calcium overload and α -synuclein aggregation in an enteroendocrine cell line. iScience. 2022;25.
54. Faghfuri E, Gholizadeh P. The role of Akkermansia muciniphila in colorectal cancer: A double-edged sword of treatment or disease progression? Biomed Pharmacotherapy. 2024;173.
55. Verdin E. NAD + in aging, metabolism, and neurodegeneration. Sci (1979). 2015;350:1208–13.
56. Kam TI, Mao X, Park H, Chou SC, Karuppagounder SS, Umanah GE, et al. Poly(ADP-ribose) drives pathologic α-synuclein neurodegeneration in Parkinson's disease. Science. 2018;362:eaat8407.
57. Love S, Barber R, Wilcock GK. Increased poly(ADP-ribosyl)ation of nuclear proteins in Alzheimer's disease. Brain. 1999;122:247–53.
58. Wencel PL, Lukiw WJ, Strosznajder JB, Strosznajder RP. Inhibition of Poly(ADP-ribose) Polymerase-1 enhances gene expression of selected sirtuins and APP cleaving enzymes in amyloid Beta cytotoxicity. Mol Neurobiol. 2018;55:4612–23.
59. Meng L, Jin H, Yulug B, Altay O, Li X, Hanoglu L, et al. Multi-omics analysis reveals the key factors involved in the severity of the Alzheimer's disease. Alzheimers Res Ther. 2024;16:213.
60. Chen YC, Lin HY, Chien Y, Tung YH, Ni YH, Gau SSF. Altered gut microbiota correlates with behavioral problems but not Gastrointestinal symptoms in individuals with autism. Brain Behav Immun. 2022;106:161–78.
61. Bui TPN, Shetty SA, Lagkouvardos I, Ritari J, Chamlagain B, Douillard FP, et al. Comparative genomics and physiology of the butyrate-producing bacterium intestinimonas butyriciproducens. Environ Microbiol Rep. 2016;8:1024–37.
62. Liu X, Mao B, Gu J, Wu J, Cui S, Wang G, et al. Blautia—a new functional genus with potential probiotic properties? Gut Microbes. 2021;13:1–21.
63. Yıldırım S, Nalbantoğlu ÖU, Bayraktar A, Ercan FB, Gündoğdu A, Velioğlu HA, et al. Stratification of the gut microbiota composition landscape across the Alzheimer's disease continuum in a Turkish cohort. mSystems. 2022;7:e0000422.
64. Aljumaah MR, Bhatia U, Roach J, Gunstad J, Azcarate Peril MA. The gut microbiome, mild cognitive impairment, and probiotics: A randomized clinical trial in middle-aged and older adults. Clin Nutr. 2022;41:2565–76.
65. Abraham D, Feher J, Scuderi GL, Szabo D, Dobolyi A, Cservenak M, et al. Exercise and probiotics attenuate the development of Alzheimer's disease in Transgenic mice: role of Microbiome. Exp Gerontol. 2019;115:122–31.
66. Zha X, Liu X, Wei M, Huang H, Cao J, Liu S, et al. Microbiota-derived lysophosphatidylcholine alleviates Alzheimer's disease pathology via suppressing ferroptosis. Cell Metab. 2024;37:169–86.
67. Frame NW, Allas MJ, Pequegnat B, Vinogradov E, Liao VCH, Al-Abdul-Wahid S, et al. Structure and synthesis of a vaccine and diagnostic target for enterocloster Bolteae, an autism-associated gut pathogen– Part II. Carbohydr Res. 2023;526:108805.
68. Enemchukwu CU, Ben-Faras H, Gialanella P, Szymczak WA, Nosanchuk JD, Madaline TF. Butyricimonas virosa bacteraemia and bowel disease: case report and review. New Microbes New Infect. 2016;13:34–6.
69. Noble EE, Olson CA, Davis E, Tsan L, Chen YW, Schade R, et al. Gut microbial taxa elevated by dietary sugar disrupt memory function. Transl Psychiatry. 2021;11:1–16.
70. Wu M, Cheng Y, Zhang R, Han W, Jiang H, Bi C, et al. Molecular mechanism and therapeutic strategy of bile acids in Alzheimer's disease from the emerging perspective of the microbiota–gut–brain axis. Biomed Pharmacother. 2024;178:117228.
71. MahmoudianDehkordi S, Arnold M, Nho K, Ahmad S, Jia W, Xie G, et al. Altered bile acid profile associates with cognitive impairment in Alzheimer's disease—An emerging role for gut Microbiome. Alzheimer's Dement. 2019;15:76–92.
72. Nho K, Kueider-Paisley A, MahmoudianDehkordi S, Arnold M, Risacher SL, Louie G, et al. Altered bile acid profile in mild cognitive impairment and Alzheimer's disease: relationship to neuroimaging and CSF biomarkers. Alzheimer's Dement. 2019;15:232–44.
73. Fernstrom JD. Branched-Chain amino acids and brain function. J Nutr. 2005;135:S1539–46.
74. Sperringer JE, Addington A, Hutson SM. Branched-Chain amino acids and brain metabolism. Neurochem Res. 2017;42:1697–709.

75. Cole JT, Mitala CM, Kundu S, Verma A, Elkind JA, Nissim I, et al. Dietary branched chain amino acids ameliorate injury-induced cognitive impairment. Proc Natl Acad Sci U S A. 2010;107:366–71.
76. Polis B, Samson AO. Role of the metabolism of branched-chain amino acids in the development of Alzheimer's disease and other metabolic disorders. Neural Regen Res. 2020;15:1460–70.
77. Tynkkynen J, Chouraki V, van der Lee SJ, Hernesniemi J, Yang Q, Li S, et al. Association of branched-chain amino acids and other Circulating metabolites with risk of incident dementia and Alzheimer's disease: A prospective study in eight cohorts. Alzheimer's Dement. 2018;14:723–33.
78. Zhang Y, He X, Qian Y, Xu S, Mo C, Yan Z, et al. Plasma branched-chain and aromatic amino acids correlate with the gut microbiota and severity of Parkinson's disease. Npj Parkinson's Disease 2022. 2022;8(1):8:1–10.
79. Schweickart A, Batra R, Neth BJ, Martino C, Shenhav L, Zhang AR, et al. Serum and CSF metabolomics analysis shows mediterranean ketogenic diet mitigates risk factors of Alzheimer's disease. Npj Metabolic Health Disease. 2024;2:15.

Publisher's note